

A method for in-situ calibration of Aanderaa oxygen sensors on surface moorings

Seth M. Bushinsky*, Steven Emerson

School of Oceanography, University of Washington, 1492 NE Boat St., Seattle, WA 98105, United States



ARTICLE INFO

Article history:

Received 9 January 2013

Received in revised form 1 May 2013

Accepted 2 May 2013

Available online 8 May 2013

Keywords:

Oxygen

Moorings buoys

Calibration

In situ measurements

ABSTRACT

Oxygen-based mass balance estimates of net biological production can be calculated using accurate in-situ O_2 measurements. All presently available oxygen sensors drift if deployed for periods of months in the sun-lit surface ocean and must be calibrated to maintain accuracy. We have developed an in-situ calibration system in which Aanderaa optode oxygen sensors periodically determine the pO_2 of air. In the moored application described here, the optode is housed in a subsurface chamber on a surface mooring where it alternately measures the pO_2 of the water and air. During calibration intervals, atmospheric air is pumped into the optode housing, displacing the water. Subsequent oxygen measurements of the air inside the housing provide a measurement of the atmospheric pO_2 , which can then be compared to expected atmospheric pO_2 based on measured pressure and temperature. We present calibrations for one optode in both water (against Winkler titrations) and air (against atmospheric oxygen). The optode response in lab experiments was different in air than in water, measuring low and exhibiting temperature dependence (-1% at $20\text{ }^\circ\text{C}$ and -2.3% at $3\text{ }^\circ\text{C}$). Initial field tests in a freshwater inlet confirmed this offset and showed a drift of -0.5% over 3 months of deployments.

© 2013 Elsevier B.V. All rights reserved.

1. Introduction

An important indicator of biogeochemical processes in the ocean is oxygen consumption and production. In-situ oxygen measurements are a key component of oxygen-based mass balance estimates of net community production and measurements of ocean respiration. Net biological oxygen production is related to net community carbon production (NCP) and biological carbon export, which is one of the dominant controls on atmospheric pCO_2 (Marinov et al., 2008; Sarmiento and Toggweiler, 1984). Capturing annual fluxes and interannual variability requires year-long measurements that can only be done through repeated observations or remotely deployed instruments (Emerson et al., 2008). Euphotic zone biological oxygen production takes place primarily in the ocean mixed layer, so the air–sea flux is the dominant term in many areas of the ocean (Nicholson et al., 2008). Because oxygen concentrations in surface waters vary only within a few percent of saturation, small inaccuracies in measurement can result in large errors in the calculation of supersaturation. Uncertainty in oxygen measurements accounts for an error of $\pm 50\%$ in carbon export estimates in the sub-tropics using an oxygen mass balance (Emerson et al., 2008). Since in-situ O_2 sensors deployed in the euphotic zone drift, it is necessary for these sensors to be calibrated during a deployment.

The use of remotely deployed oxygen sensors has recently expanded as moorings, gliders, and profiling floats incorporate sensors to better determine biogeochemical cycles (Emerson et al., 2008; Emerson and

Stump, 2010; Nicholson et al., 2008; Johnson et al., 2009; Riser and Johnson, 2008). Remote locations and increasing lengths of deployment magnify the need for calibration. While good stability has been shown for floats that spend much of their time in dark, low-productivity waters (Körtzinger et al., 2005; Riser and Johnson, 2008), even these data have not been exploited for determining the exchange between the air and water because of uncertain accuracy. Oxygen sensors on profiling floats have been calibrated with climatological oxygen values at depth (Martz et al., 2008), but this method is not accurate enough to determine small departures from saturation in surface waters. In this paper we describe an in-situ oxygen calibration system designed to work on surface moorings using Aanderaa optode oxygen sensors.

Optodes manufactured by Aanderaa Data Instruments (Tengberg et al., 2003) utilize the oxygen-mediated luminescent response of a platinum porphyrin compound embedded in a silicone foil to measure oxygen. Optodes respond to the partial pressure of oxygen and have been shown to work in gasses as well as seawater (Bacon and Demas, 1987; Stokes and Somero, 1999). When a blue-green (505 nm wavelength) light emitting diode illuminates and excites the foil, a red luminescence is generated as the excited molecules return to their original ground energy state (Tengberg et al., 2006). The presence of oxygen quenches this reaction, as energy is transferred to oxygen molecules instead of being released as photons. Both the intensity and the duration, or lifetime, of luminescence is dependent on the partial pressure of oxygen and the temperature. While some oxygen sensors measure the intensity, which requires simpler electronics, the intensity response to oxygen is more prone to drift due to photo bleaching (Tengberg et al., 2006). Instead, Aanderaa optodes measure changes in luminescence

* Corresponding author. Tel.: +1 206 543 1355.

E-mail address: smbush@u.washington.edu (S.M. Bushinsky).

lifetime of the light emitted by the foil. The phase of the emitted light is shifted relative to the excitation light and this shift is related to the lifetime of fluorescence and therefore pO_2 . Measuring phase shift requires more expensive sensors and computation but provides greater stability (Demas et al., 1999). Calibration problems with Aanderaa optodes have been noted and in-situ calibrations using discrete water samples have been used to improve oxygen measurements from shipboard casts (Uchida et al., 2008). An initial calibration provides good accuracy; however, for longer deployments where subsequent calibrations are impractical an in-situ calibration system is preferred.

Using atmospheric oxygen as a standard (Körtzinger et al., 2005) requires knowing the mole fraction of oxygen in the air, $X_{O_2} = 0.20939$ (Khélifa et al., 2007), atmospheric pressure, P_{Atm} , and temperature. The partial pressure of oxygen is related to these values by:

$$pO_2^{atmos} = (P_{Atm} - p_{H_2O})X_{O_2} \quad (1)$$

where p_{H_2O} is the partial pressure of the water vapor and is a function of relative humidity and temperature. The instrument we describe makes accurate pressure and temperature measurements in an atmosphere that is fully saturated with water. Therefore, in our calculations, the relative humidity is assumed to be 100%, and p_{H_2O} in fresh water varies with temperature according to the Goff–Gratch equation (Goff and Gratch, 1946). While the Aanderaa oxygen-sensitive luminescent compounds have been shown to respond similarly in gasses and water, previous work has only established that the response is equivalent to within several percent (Bacon and Demas, 1987). Calibrations to better than a percent are necessary for this system.

2. Methods

2.1. Laboratory optode calibrations

Calibration of an Aanderaa 4330F fast response optode with a digital to analog converter was performed against Winkler titrations in a 75 L insulated water tank with 80% of the water surface covered to reduce gas exchange. Calibrations were made in fresh water across a range of five temperatures between 3 and 20 °C and at least five oxygen saturation states between 50 and 130%. Temperature was maintained to within ± 0.05 °C using temperature controlled water pumped through copper tubing inside the water tank. Oxygen concentration was increased by bubbling pure oxygen or decreased by bubbling pure nitrogen (Fig. 1). Water inside the bath was continuously mixed and gas bubbling was stopped for 20 min prior to water sampling in order to allow the optode measurement (pO_2^{optode}) to stabilize (Fig. 2). Once stabilized, the optode showed a measurement precision of $\pm 0.1\%$ std. dev. Replicate Winkler samples were taken during a 2–2.5 minute time interval at every oxygen saturation level. Samples were titrated manually to a visual endpoint using a Metrohm autoburette and standardized against a WAKO KIO_3 solution (Emerson et al., 1999; Carpenter, 1965). Optode measurements were taken every 10 s and averaged over the time period during which the Winkler replicates were collected.

The response of the optode in air was determined by placing it in an airtight chamber below the water line in the same temperature controlled tank (Fig. 3). Air was pumped into the chamber, completely evacuating the water, and trapped for 3 h. During this time, the air temperature was recorded using the optode's thermistor and air pressure in the chamber was measured using a Paroscientific Model 223A-102 Pressure Transducer (repeatability and hysteresis to $\pm 0.005\%$, Payne, 1995). pO_2^{atmos} measurements were made at temperatures between 3 and 20 °C. The optode sample rate was slowed to once every 60 s for the air measurements to avoid self-heating.

While lab air has approximately 35% relative humidity, inside the air calibration chamber the air became saturated within the time it took for the air temperature to come into equilibrium with the surrounding water (<2 min). This was confirmed by pumping air into the chamber

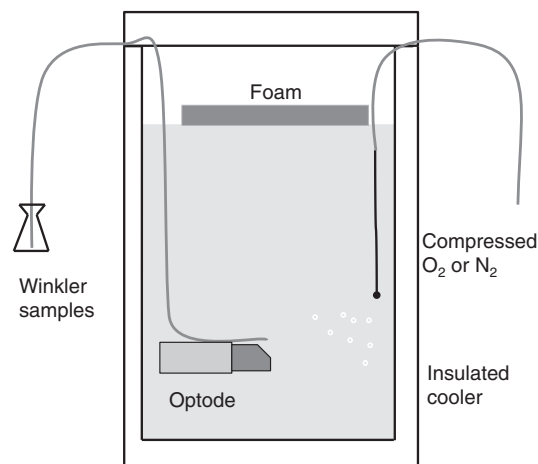


Fig. 1. Schematic of the lab setup used to calibrate Aanderaa optodes. The water bath is continuously circulated and temperature controlled. The optode phase measurement (P_r) was recorded every 10 s throughout each experiment. Water for Winkler titrations was sampled at 5 or more oxygen saturation levels between 50 and 130%. The foam covering the water surface was free floating so that as water was removed for Winkler samples it stayed at the surface and continued to suppress gas exchange.

that had been passed through Drierite (anhydrous $CaSO_4$) or bubbled through a water-submerged frit and monitoring pO_2^{optode} and pressure measurements in the trapped air over time. No detectable difference was observed between the optode measurements in dried or moistened air. Furthermore, after the temperature stabilized, pO_2^{optode} and pO_2^{atmos} remained constant, indicating that the water vapor pressure was saturated (at equilibrium).

2.2. In-situ O_2 calibration system

The in-situ calibration system consists of: a submerged Sea-Bird CTD (SBE 16) with water pump and Aanderaa oxygen sensor, and an above-surface electronics housing, which controls the timing of the calibration

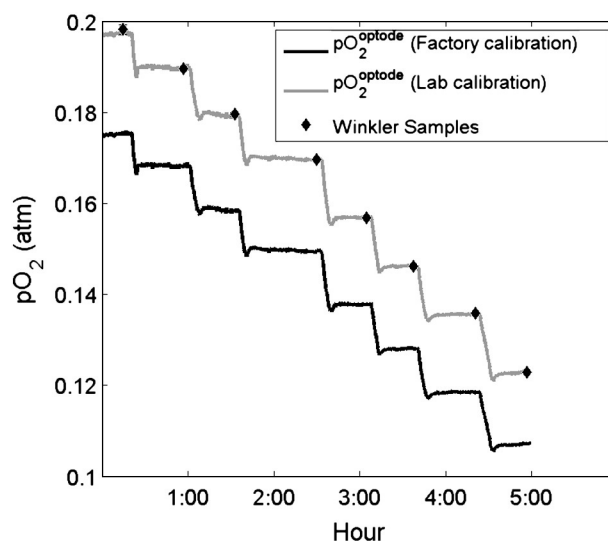


Fig. 2. Example of oxygen change during a water calibration experiment at 20 °C. pO_2^{optode} using factory calibration (black line) is significantly lower than pO_2^{optode} derived from the lab calibration (gray). Winkler titrations for this experiment are the diamonds. Error bars (± 1 standard deviation) are too small to see, except for the highest pO_2 Winkler sample. This data point had a 0.55% standard deviation between Winkler replicates and was therefore removed from the calculation of the surface fit.

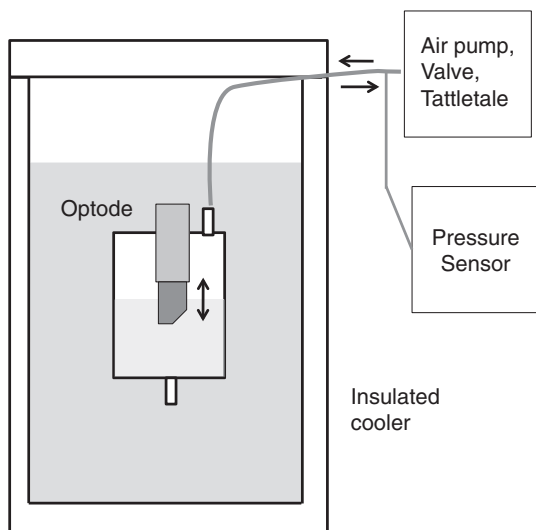


Fig. 3. Schematic of lab setup used to determine air response of the optode. Water bath is temperature controlled and continuously circulated. Air was pumped into the optode housing and trapped for 3 h, during which the pressure was measured every 10 s and the optode sampled every minute in the air. This was repeated at least 5 times at each temperature.

cycles and contains the pumps and valves necessary to drive air into the optode housing (Fig. 4). The SBE 16 is set to take measurements on a regular time interval. Prior to each measurement, the water pump is switched on for 20 s before the temperature, salinity, pO_2^{optode} and optode temperature are recorded. The optode is housed inside a sealed PVC cylinder with three openings, two on either side to allow water to

enter and exit and one on top to allow air to enter and exit. To limit bio-fouling, tributyl tin inserts are placed in multiple locations along the water tubing and the optode chamber is lined with copper.

An air hose connects the air pump, air valves, and pressure sensor in the electronics housing with the optode compartment. Inside the electronics housing a Tattletale-4A (Onset Computer Corporation), controls an air pump, air valves, and a GE Druck RPT-200 pressure sensor (accuracy $\pm 0.01\%$). The water pump, pressure sensor, and optode are electronically connected to both the SBE 16 and the Tattletale. The Tattletale monitors the voltage of the power cable between the SBE 16 and the water pump, removing the need to synchronize clocks between the SBE 16 and the Tattletale, as the Tattletale can count SBE 16 sample cycles to determine when to start an air calibration period. The pressure sensor and optode are recorded both by the SBE 16 and the Tattletale. The SBE 16 only records one measurement after the 20 s of pumping, while the Tattletale can record oxygen and pressure at a user-defined frequency. The entire system is packaged to fit on a surface mooring (Fig. 4) and designed for future deployment at Ocean Station Papa in the Northeast Pacific (50 N, 145 W; Emerson and Stump, 2010).

After a pre-determined number of water samples, the Tattletale initiates an air calibration period in which air is pumped from the atmosphere into the optode housing, displacing the water and flushing the air lines and housing over 4 times before a valve is closed and the air is trapped. After the temperature comes to equilibrium, pO_2^{optode} , air pressure, and temperature are measured in the trapped air. Because the optode response time is 8–28 s and the pressure sensor response time is less than a second, wave activity could cause changes in the air pressure that are not reflected in the optode measurement. To average out the effect of short-term changes in pressure, multiple optode and pressure measurements are made to allow accurate comparison of pO_2^{optode} to pO_2^{tmos} .

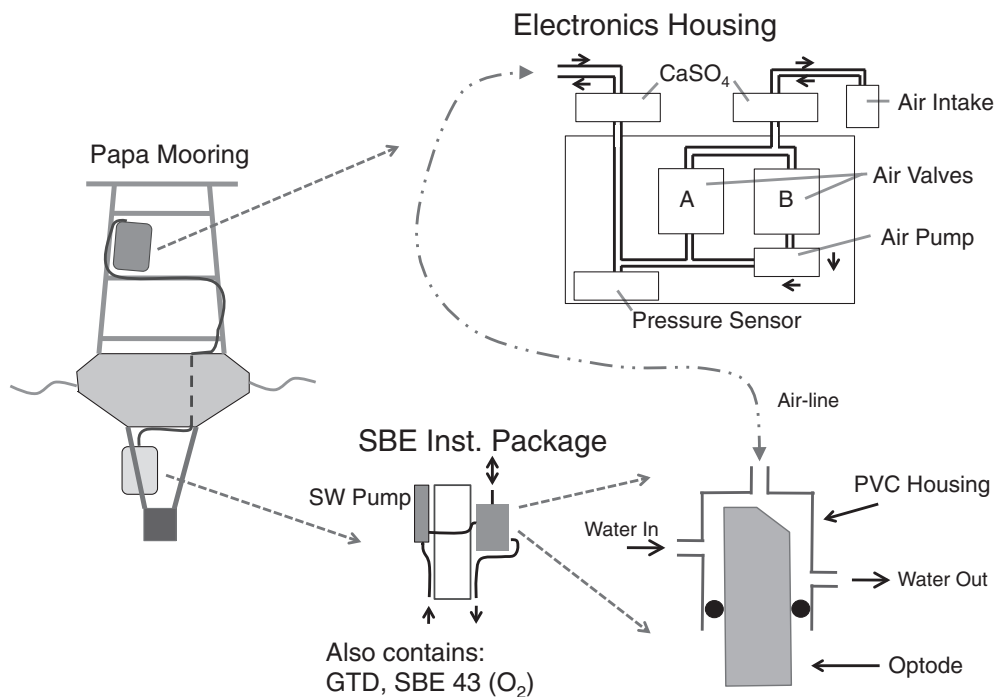


Fig. 4. Schematic of calibration system for mooring deployment. The in-situ calibration system consists of a subsurface instrument package and a tower-mounted electronics housing. The subsurface instrument package contains the SBE 16 CTD, water pump, and optode. The electronics housing contains the Tattletale-4A controlling computer, pressure sensor, air pump, and valves. At the start of a calibration period, the latching air valve (A) closes, the solenoid air valve (B) opens, and the air pump pushes air down into the optode housing. When the air pump stops, the solenoid air valve closes, trapping air in the optode housing. The pressure sensor is always connected to the air-line going down to the optode housing and measures the pressure at the same time that the optode takes samples. $CaSO_4$ chambers are positioned in-line with tubing going to both the atmosphere and down to the optode housing. These trap moisture to prevent condensation inside the tubing within the electronics housing. The air intake is designed to prevent rain or waves from flooding the tubing by physically slowing water flow into the tube through a nested set of cylinders punctured by small holes. The air intake will be positioned on the upper portion of the mooring tower to limit the amount of time it can be submerged by waves. Lab tests show that the intake housing can withstand ~5 s of full submersion while the air pump is running without allowing water to reach the air line.

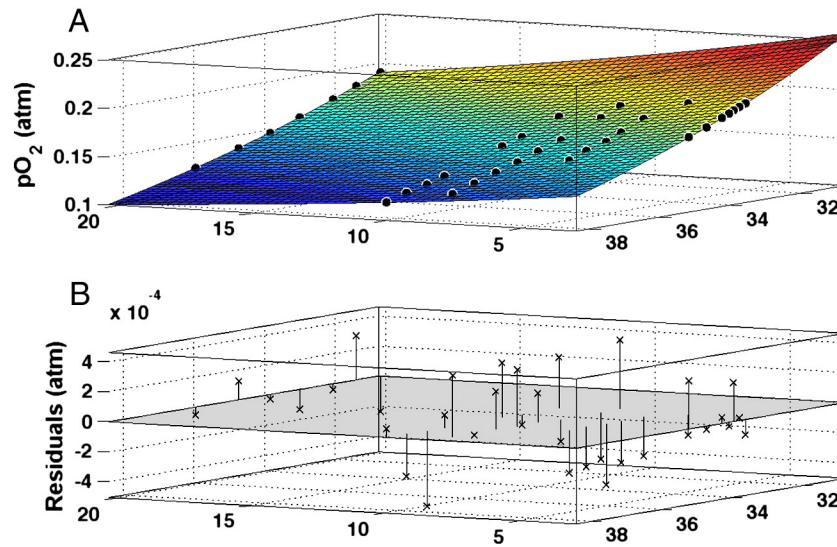


Fig. 5. Calibration data from multiple oxygen concentrations at multiple temperatures. The fitted surface (A) has an RMS error of 0.00028 (atm). Data were fit to the Eqs. (2)–(5) and coefficients were calculated using the Matlab Surface Fitting Toolbox. Residuals (B) were calculated and calibration points were filtered to include only those with residuals within two standard deviations of the mean of the residuals. A and B show the 35 points used for the fit; 8 calibration points were removed after failing the Winkler replicate standard deviation (5 points) threshold of 0.2% or the residual filtering (3 points).

3. Results

3.1. Water calibration

The optode response to pO_2 and temperature was formulated using the Surface Fitting Toolbox from Matlab. pO_2^{optode} was calculated using a Stern–Volmer based equation presented in Uchida et al. (2008):

$$pO_2^{\text{optode}} = \left(\frac{P_0}{P_c} - 1 \right) / K_{SV} \quad (2)$$

$$K_{SV} = C_0 + C_1 T + C_2 T^2 \quad (3)$$

$$P_0 = C_3 + C_4 T \quad (4)$$

$$P_c = C_5 + C_6 P_r \quad (5)$$

where P_r represents the raw optode phase shift, P_0 represents the optode phase shift in anoxic water, and K_{SV} is the Stern–Volmer constant. C_{0-6} were calculated from the correlations among the optode phase shift (P_r), Winkler-derived pO_2 , and temperature (T) (Fig. 5A). Zero O_2 measurements were not used for this calibration because all oxygen concentrations in the data collected for this study were near saturation. Addition of zero O_2 calibration points affect calculation of near saturation oxygen values by less than 0.05%. Prior to fitting, optode measurements and Winkler replicates with a percent standard deviation greater than $\pm 0.2\%$ were removed from the calibration (5 points removed out of 43). Residuals between Winkler pO_2 and the fitted surface were calculated

(Fig. 5B), and if any residuals fell outside of 2 standard deviations from the mean, the calibration point with greatest residual was removed. The data were iteratively fit to the equation, successively filtering out high residuals until all residuals fell within 2 standard deviations (3 additional points removed, leaving 35 for the fit). The resulting surface fit had a RMS error of ± 0.00028 atm ($\sim 0.13\%$ of atmospheric pO_2).

3.2. Laboratory air response and calibration

Once calibrated in water, the optode was repeatedly exposed to air across a range of temperatures (Table 1). For each air period at a given temperature, pO_2^{optode} stabilized within 2 min and was repeatable for each air period. Between 5 and 12 air cycles were run for each temperature. pO_2^{optode} measurements in air (Fig. 6) were compared to pO_2^{atmos} calculated from T , P and pH_2O Eq. (1). During each air period, pO_2^{optode} was lower than pO_2^{atmos} . The difference between pO_2^{optode} and pO_2^{atmos} changed with temperature. At 20 °C, pO_2^{optode} measured 1% lower than pO_2^{atmos} , while at 3 °C, pO_2^{optode} measured 2.3% below pO_2^{atmos} .

Water pO_2^{optode} measured in between air periods (the short periods of lower pO_2) showed changes consistent with the cooling water temperature (Fig. 6). When the water is cooled during a temperature change, the pO_2 drops due to the initial undersaturation of the colder water. As oxygen invades the water bath, the pO_2 of the water rises. This initial undersaturation was considered as a possible source of error, due to the possibility that diffusion of oxygen from the trapped, pressurized air to the undersaturated water was the cause of the low pO_2 measured by the optode. The more undersaturated water remaining on the walls or base of the chamber, the more oxygen could diffuse

Table 1
List of important experiments.

Purpose	Temperature range (°C)	Duration (days)	Sample interval (seconds)	Number of calibration cycles	Num. of individual points averaged for each cal. cycle avg. (Figs. 9/10)
Water calibration	3–20	5	10	–	–
Air response	3–20	7	60	27	26
Effect of initial rel. humidity on air response	2, 20	4	10	–	–
Dock test: 2011-03-14	7–8	4	900	10	4
Dock test: 2011-04-14	8–10	5	600	23	3
Dock test: 2011-04-19	10–11	3	180	6	9
Dock test: 2011-05-30	13–15	4	600	18	2
Dock test: 2011-06-02	14–18	26	1200	128	1

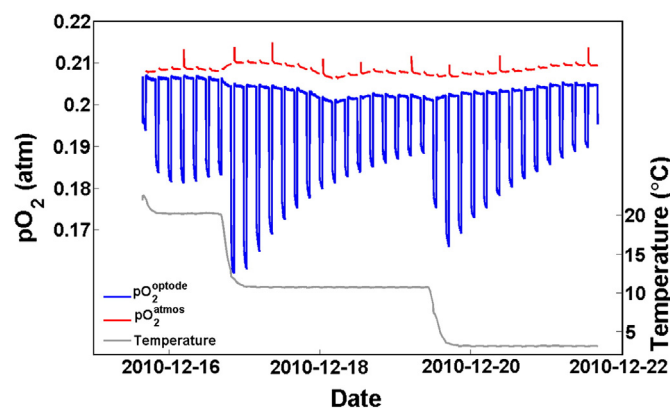


Fig. 6. Calibrated pO_2^{optode} (blue, middle plunging line) over multiple 3-h cycles between air and water in the laboratory. Air periods correspond to the high plateaus in the optode plot and water immersion to the shorter, low pO_2 periods. Over a temperature (gray, bottom line) range of 20–3 °C the optode measured between –1% and –2.8% below calculated pO_2^{atmos} (red, top broken line). (For interpretation of the references to color in this figure legend, the reader is referred to the web version of this article.)

out of the air. However, the chamber was designed to drain completely with the minimum surface area of water exposed to the air. Calculations show that even in an extreme case where the water temperature changed instantly from 20 to 5 °C, the impact on the pO_2 in the air would be less than 0.1%. In the lab and field experiments shown here, the temperature changes were far slower and the effect therefore much smaller.

The difference between pO_2 measured by the calibrated optode (pO_2^{optode}) and that calculated from Eq. (1) is expressed as a percent difference in Fig. 7, where negative values indicate the optode reading lower than pO_2^{atmos} . Error bars show ± 1 standard deviation for an average of 25 min of sampling during each air period.

The reasons for the different optode response in air and water are unknown and need to be better understood. We considered the possibility that the optode chamber did not reach 100% relative humidity, which would cause pO_2^{atmos} to be too high relative to pO_2^{optode} . While water vapor pressure is in the range of the magnitude of offset observed, if the air started out undersaturated with water vapor, we would expect that given enough time the humidity in the optode chamber would eventually rise towards full saturation and the offset would disappear; instead, the offset between pO_2^{optode} and pO_2^{atmos} remained stable, despite air periods of up to 20 h.

Another potential reason considered for the difference in optode measurement between air and water is that the refractive indexes of air and water are different. The optode used in this study does not have a silicon coating over the foil and could be more susceptible to different measurements in air and water. The possibility also remains that oxygen interacts differently with the platinum porphyrin compound in

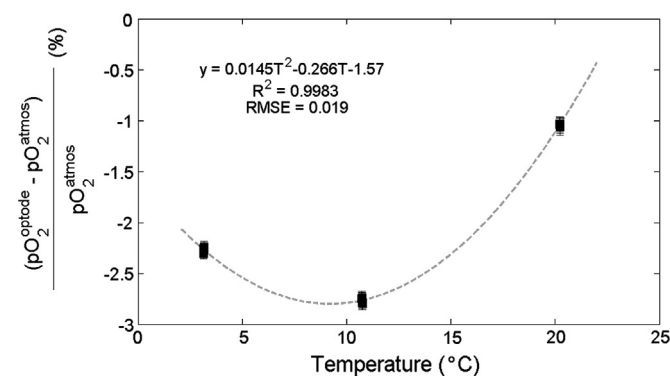


Fig. 7. Temperature dependence of the difference between calibrated optode atmospheric pO_2 and the true value. Percent difference is calculated as $((pO_2^{\text{optode}} - pO_2^{\text{atmos}}) / pO_2^{\text{atmos}}) \times 100$. Error bars are ± 1 standard deviation.

the foil when exposed to different media, perhaps due to interactions on a molecular level.

3.3. Tests of the in-situ instrument

The field calibration system was tested off the dock of the Marine Sciences Building at the University of Washington in Portage Bay, a sheltered freshwater inlet. Five calibration runs were performed over 3–26 day periods in which the optode was exposed to air for 3 h then submerged in water for 1 h. The SBE 16 recorded the optode and pressure sensor on intervals ranging from 3 to 20 min (Table 1). These tests were designed to replicate sample cycles similar to those on a mooring-mounted Sea-Bird instrument package and O_2 sensor currently deployed at Station Papa. This mooring is the intended initial deployment location for this calibration system and takes measurements at a frequency of once every 3 h.

An average of the uncorrected pO_2^{optode} measurements from the beginning of each 3-h calibration period was plotted for all experiments (Fig. 8). These data have a greater spread than laboratory data, but indicate the same overall temperature dependence. In order to use atmospheric pO_2 to calibrate optodes in-situ, the temperature dependent offset measured in the lab (Fig. 7) must be removed from the optode measurements in the air to obtain $pO_2^{\text{optode,corr}}$:

$$pO_2^{\text{optode,corr}} = pO_2^{\text{optode}} \times \left(\frac{-y}{100} + 1 \right) \quad (6)$$

where y is the temperature dependent correction based on the polynomial fit shown in Fig. 7. From these corrected samples, the percent difference between $pO_2^{\text{optode,corr}}$ and pO_2^{atmos} was computed at each time point (Fig. 9).

Several factors could be responsible for the increased variability of the field data. The pressure sensor has a response time of less than 1 s, while the response time of the optode is 8–28 s. If the total pressure in the housing changed rapidly enough, the fast response time of the pressure sensor could result in offsets between $pO_2^{\text{optode,corr}}$ and pO_2^{atmos} . Pressure changes could result from trends in atmospheric pressure or temperature, or passing waves. Atmospheric changes would be unlikely to occur quickly enough to exploit the difference in instrument response times. Passing waves are a more likely source of error. A wave or wake passing over the calibration system could cause a transient change in pressure that would be measured by the pressure sensor but which would be transient or damped in the optode reading. In these field tests the calibration system was attached to a fixed dock and was therefore more susceptible to wave-induced pressure fluctuations than it would be on a floating mooring. Calculations of the pressure effect of typical passing waves indicate that the additional error in the oxygen measurement would be below 0.01%.

Difficulties in maintaining pressurization of the optode chamber also were likely a cause of some of the variability present in the field data. Slow air leaks from the system caused the drops in $pO_2^{\text{optode,corr}}$ seen in Fig. 9 during many of the air periods. Several small weak points in the design were subsequently identified and corrected.

The advantage of taking multiple measurements during each calibration period and having frequent calibration periods during each deployment is that the noise in the air measurements can be averaged out. Between 1 and 9 individual calibration measurements were averaged for each calibration period during the field tests (Table 1), greatly reducing the spread in the data. The batteries and memory space in the electronics housing and Tattletale can provide power and storage to run the calibration system once per day for approximately 6 years, far longer than the SBE 16 batteries could last. Therefore, frequent air calibrations can be performed throughout a deployment, reducing the uncertainty introduced by variations in the field environment.

Correcting all field data for the air response removes the temperature dependence of the air response (Fig. 10). Averaging multiple

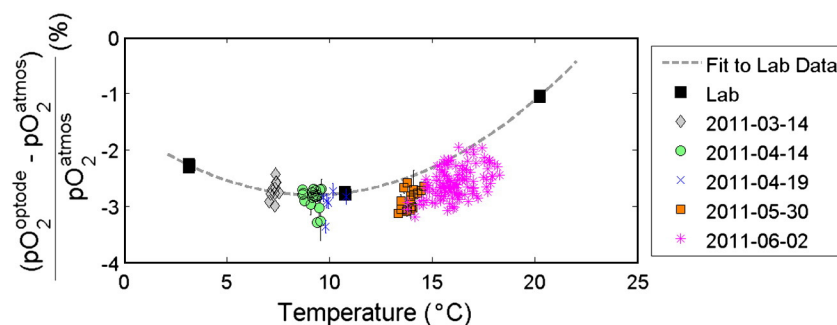


Fig. 8. Data from Portage Bay dock experiments (colored symbols) overlaid on lab data. Best fit to lab data is the polynomial fit shown, which gives $y = 0.0145T^2 - 0.266T - 1.57$. This fit was used in Eq. (6) to correct dock experiment data to eliminate the calibration offset in air (Figs. 9 and 10). Field test 6/02/2011 had a significant air leak, allowing air to leave the optode chamber quickly during the calibration periods. Therefore, only the first air measurement was used for each air period and no error bars are displayed for the data shown here. (For interpretation of the references to color in this figure legend, the reader is referred to the web version of this article.)

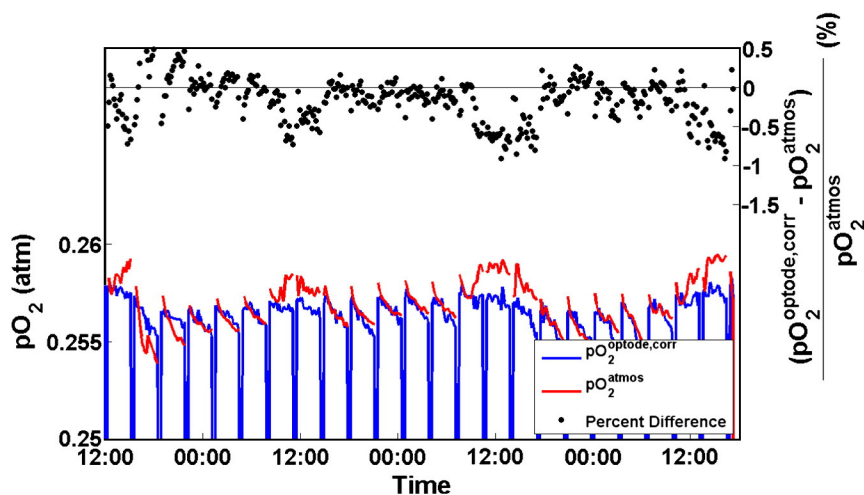


Fig. 9. Example of a field test of the optode calibration system. pO_2^{atmos} (red) is compared to the calibrated and air corrected optode data, $pO_2^{\text{optode,corr}}$ (blue). Percent difference is shown in black dots.

calibration cycles removes the spread in the data and brings the calibration to $\pm 0.1\%$, allowing the determination of subsequent drift during a deployment. The apparent temperature dependence that remains in Fig. 10 indicates a 0.5% drift in the 3 months between the first and last field experiments, which would be much faster than previously reported; however, no drift data has been published for a fast response optode. Additional lab calibrations performed 2 months after the last field experiment shown in Fig. 10 confirmed this drift and showed it continued in the same direction to a shift of $\sim 2\text{--}3\%$

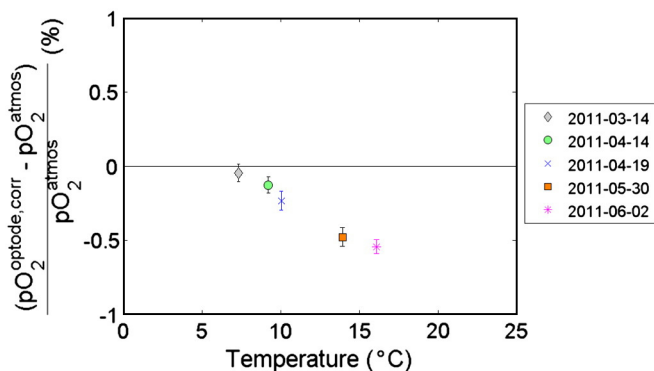


Fig. 10. After removing the air calibration offset observed in the lab, the Portage Bay data are shown here as the percent difference from pO_2^{atmos} . Error bars indicate ± 2 standard errors. Temperature measurements have an error of $\pm 0.02\%$.

between lab calibrations 9 months apart. The lack of an optical isolation layer may make this sensor much more vulnerable to photo-bleaching and cause more rapid drift.

4. Conclusions

The in-situ optode calibration system is capable of making in-situ oxygen measurements in air to $\pm 0.1\%$. This technique shows promise for increasing the utility of long-term deployments of oxygen sensors through repeated calibrations over their lifetime. Moorings provide an ideal platform for this system, with ample space for the pressure sensor, air pumps, valves, controlling computer, and batteries needed to pump air subsurface and record accurate air pressure.

Looking forward, there are several challenges that need to be addressed both in the lab and field. The temperature dependent offset in air can be accommodated, as shown in this study, as long as it remains stable and consistent. For this instrument's planned deployment in the northeast Pacific characterization of the air offset from 3 to 20 °C was sufficient; however, in the future an examination of the response in air across a wider range of temperatures may yield more information about the cause of the offset. In order to use this calibration technique to correct for drift in the water measurements, an exactly equal drift must occur in the air response, but long-term stability of these optodes in the air is not known.

The temperature and oxygen sensitivity of the sensing foil require a multi-point calibration in the lab, but this remains impractical for field deployments. This calibration technique provides 1 calibration

point that can be used to shift the calibration surface but not completely replace the initial calibration data. The advantage of using atmospheric air for the sole calibration point is that pO_2^{atmos} is within a few percent of the surface water oxygen concentration, thus optimizing the accuracy in determining the air–water concentration difference.

The main advantage of using a mooring for this technique is the ability to mount an accurate pressure sensor for calculating pO_2^{atmos} . If accurate pressure can be obtained from reanalysis products or nearby moorings, this technique can be expanded to profiling floats or gliders. As more elements of a biogeochemical sensor network are deployed for longer periods of time, it will become ever more important to perform in-situ calibrations on oxygen sensors.

Acknowledgments

This work was supported by the National Science Foundation under grant OCE 0850286. The calibration system electronics and air pumping system were designed, built, and tested by Peter Kauffman. Randy Fabro, Tor Bjorklund, and Steven Elliot of UW Fabrication and Engineering Services provided essential fabrication and construction guidance. Diane Perry and Evan Howard greatly assisted the lab calibrations. Charles Stump gave all around guidance and assistance throughout the course of this work. An anonymous reviewer provided suggestions that greatly improved the clarity of this manuscript.

References

- Bacon, J.R., Demas, J.N., 1987. Determination of oxygen concentrations by luminescence quenching of a polymer-immobilized transition-metal complex. *Anal. Chem.* 59, 2780–2785.
- Carpenter, J.H., 1965. The Chesapeake Bay Institute technique for the Winkler dissolved oxygen method. *Limnol. Oceanogr.* 10, 141–143.
- Demas, J.N., DeGraff, B.A., Coleman, P.B., 1999. Oxygen sensors based on luminescence quenching. *Anal. Chem.* 71, 793A–800A.
- Emerson, S., Stump, C., 2010. Net biological oxygen production in the ocean—II: remote in situ measurements of O_2 and N_2 in subarctic pacific surface waters. *Deep-Sea Res. I* 57, 1255–1265.
- Emerson, S., Stump, C., Wilbur, D., Quay, P., 1999. Accurate measurement of O_2 , N_2 , and Ar gases in water and the solubility of N_2 . *Mar. Chem.* 64, 337–347.
- Emerson, S., Stump, C., Nicholson, D., 2008. Net biological oxygen production in the ocean: remote in situ measurements of O_2 and N_2 in surface waters. *Global Biogeochem. Cycles* 22.
- Goff, J.A., Gratch, S., 1946. Low-pressure properties of water from -160 to 212 °F. *Trans. Am. Soc. Heat. Ventilating Eng.* 125–164.
- Johnson, K.S., Berelson, W.M., Boss, E.S., Chase, Z., Claustre, H., Emerson, S.R., et al., 2009. Observing biogeochemical cycles at global scales with profiling floats and gliders: prospects for a global array. *Oceanography* 22, 216–225.
- Khélifa, N., Lecollinet, M., Himbert, M., 2007. Molar mass of dry air in mass metrology. *Measurement* 40, 779–784.
- Körtzinger, A., Schimanski, J., Send, U., 2005. High quality oxygen measurements from profiling floats: a promising new technique. *J. Atmos. Oceanic Tech.* 22, 302–308.
- Marinov, I., Follows, M., Gnanadesikan, A., Sarmiento, J.L., Slater, R.D., 2008. How does ocean biology affect atmospheric pCO_2 ? Theory and models. *J. Geophys. Res.* 113.
- Martz, T.R., Johnson, K.S., Riser, S.C., 2008. Ocean metabolism observed with oxygen sensors on profiling floats in the South Pacific. *Limnol. Oceanogr.* 53, 2094–2111.
- Nicholson, D., Emerson, S., Eriksen, C.C., 2008. Net community production in the deep euphotic zone of the subtropical North Pacific gyre from glider surveys. *Limnol. Oceanogr.* 53, 2226–2236.
- Payne, R.E., 1995. Long-term stability of some barometric pressure sensors. *J. Atmos. Oceanic Tech.* 12, 182–189.
- Riser, S.C., Johnson, K.S., 2008. Net production of oxygen in the subtropical ocean. *Nature* 451, 323–325.
- Sarmiento, J.L., Toggweiler, J.R., 1984. A new model for the role of the oceans in determining atmospheric pCO_2 . *Nature* 308, 621–624.
- Stokes, M.D., Somero, G.N., 1999. An optical oxygen sensor and reaction vessel for high-pressure applications. *Limnol. Oceanogr.* 44, 189–195.
- Tengberg, A., Hovdenes, J., Barranger, D., Brocandel, O., Diaz, R., Sarkkula, J., et al., 2003. Optodes to measure oxygen in the aquatic environment. *Sea Technol.* 44, 10–15.
- Tengberg, A., Hovdenes, J., Andersson, H.J., Brocandel, O., Diaz, R., Hebert, D., et al., 2006. Evaluation of a lifetime-based optode to measure oxygen in aquatic systems. *Limnol. Oceanogr. Methods* 4, 7–17.
- Uchida, H., Kawano, T., Kaneko, I., Fukasawa, M., 2008. In situ calibration of optode-based oxygen sensors. *J. Atmos. Oceanic Tech.* 25, 2271–2281.